




RESEARCH LETTER

Adipocyte-specific CDK7 ablation leads to progressive loss of adipose tissue and metabolic dysfunction

Yizhe Chen^{1,2} , Eric Aria Fernandez¹, Catherine Roger¹, Isabel C. Lopez-Mejia¹, Lluís Fajas Coll^{1,3}  and Honglei Ji^{1,4} 

¹ Center for Integrative Genomics, University of Lausanne, Switzerland

² College of Animal Science and Technology, Northwest A&F University, Yangling, China

³ Institut National de la Santé et de la Recherche Médicale (Inserm), Languedoc Roussillon, France

⁴ Institute for Diabetes and Cancer, Helmholtz Center Munich, Neuherberg, Germany

Correspondence

H. Ji, Institute for Diabetes and Cancer (IDC), Helmholtz Munich, 85764 Neuherberg, Germany
 Tel: +49 1625864400
 E-mail: honglei.ji@helmholtz-muenchen.de

(Received 24 January 2022, revised 1 March 2022, accepted 4 March 2022, available online 30 March 2022)

doi:10.1002/1873-3468.14335

Edited by Michael Brunner

Adipose tissue regulates whole-body energy homeostasis. Both lipodystrophy and obesity, the extreme and opposite aspects of adipose tissue dysfunction, result in metabolic disorders: insulin resistance and hepatic steatosis. Cyclin-dependent kinases (CDKs) have been reported to be involved in adipose tissue development and functions. Using adipose tissue-specific knockout mice, here we demonstrate that the deletion of CDK7 in adipose tissue results in progressive lipodystrophy, insulin resistance, impaired adipokine secretion and downregulation of fat-specific genes, which are aggravated on high-fat diet and during ageing. Our studies suggest that CDK7 is a key regulatory component of adipose tissue maintenance and systemic energy homeostasis.

Keywords: adipose tissue; cyclin-dependent kinase 7; lipid metabolism; lipodystrophy

Adipose tissue plays an essential role in regulating systemic energy metabolism and glucose homeostasis. One of the functions of white adipose tissue (WAT) is to store neutral lipids in the form of unilocular lipid droplets (LDs) in adipocytes [1]. In addition, as an active endocrine organ, WAT secretes a variety of adipokines, such as adiponectin, leptin and resistin, which regulate whole-body energy homeostasis [2–5]. Whole-body adiposity could be considered an important regulator of metabolic health. Indeed, the excess of body fat deposition is causative of obesity and type 2 diabetes, while the abnormal absence of adipose tissue leads to extreme forms of metabolic dysfunction (or disorder) called lipodystrophies, which are accompanied by insulin resistance, liver steatosis and hypertriglycerolaemia [6,7]. Lipodystrophy can be divided into two main

types: genetic and acquired [8,9], which can be further classified as generalized and partial [10].

Cyclin-dependent kinases function by interacting with their cyclin subunits [11]. CDK/cyclin complexes play important roles in regulating cell cycle and transcription [12]. Mammalian CDK7, cyclin H and ménage à trois-1 (MAT1) form the Cdk-activating kinase (CAK) complex, which phosphorylates and activates other CDKs that are involved in the cell cycle progression [13,14]. In addition, CDK7 is also an essential submodule of the transcription factor IIH (TFIIH), which is responsible for the RNA polymerase II C-terminal domain (RNAPII CTD) phosphorylation and the initiation of transcription [15].

We and others have documented that the function of cyclins, CDKs and other cell cycle regulators is not limited

Abbreviations

CAK, cdk-activating kinase; CDKs, cyclin-dependent kinases; CLAMS, comprehensive laboratory animal monitoring system; E2F1, E2F transcription factor 1; EE, energy expenditure; GTT, glucose tolerance test; HFD, high-fat diet; ITT, insulin tolerance test; LDs, lipid droplets; NEFA, nonesterified fatty acid; pgWAT, perigonadal white adipose tissue; RB, retinoblastoma; RER, respiratory exchange ratio; scWAT, subcutaneous white adipose tissue; TFIIH, transcription factor IIH; TG, triacylglycerol; WAT, white adipose tissue.

to the control of cell division and proliferation [16–19]. This is the case for CDK4, a target of CDK7 that controls adipocyte differentiation [20] and the physiology of WAT through the regulation of the insulin signalling pathway [21]. Similarly, the deletion of cyclin D3, which is the regulatory subunit of CDK4, also results in decreased adipose tissue mass [22]. Moreover, it has been shown that CDK4 participates in the regulation of BAT thermogenesis by modulating the sympathetic nervous system [23]. Examples of other cell cycle regulators that participate in the regulation of metabolism include the E2F transcription factor 1 (E2F1). E2F1 regulates the expression of the PPAR γ gene during the clonal expansion phase of adipogenesis and thus promotes adipose tissue differentiation [24]. Some studies also involved E2F1 in adipose tissue biology, demonstrating that E2F1 expression is increased in the adipose tissue of obese human subjects and correlated with insulin resistance [25]. E2F1 expression was also increased in the visceral adipose tissue of mice fed a HFD and in leptin-deficient (*ob/ob*) mice [26]. On the opposite side of positive effectors of cell cycle regulation are the inhibitors of E2F and CDK activities, such as the retinoblastoma (RB) and the INK4 family members, respectively. The participation of these factors in adipose tissue physiology is, however, more controversial since both positive and negative effects have been reported [27,28].

We showed previously that CDK7 is required for beta-adrenergic agonist-induced adipose tissue browning [29], which points to an important function of this protein in adipose tissues. The role of CDK7 in white adipose tissue expansion under anabolic conditions, however, has not been reported. In this study, using an adipocyte-specific CDK7 knockout mouse model, we find that CDK7 is required for normal adipose tissue maintenance and systemic metabolism *in vivo*, especially during ageing and under diet-induced obesity.

Materials and methods

Mice

The generation of *Cdk7^{flox/flox}* and *Cdk7^{ΔKO}* mice was reported in a previous study [29]. Mice were maintained in a temperature-controlled animal facility with a 12-h light/12-h dark cycle and had access to standard chow (KLIBA NAFAG, no. 3436, Kaiseraugst, Switzerland) and water according to Swiss Animal Protection Ordinance (OPAn). HFD studies were conducted by feeding mice a purified-ingredient diet composed of 60 : 20 : 20 kcal percentage of fat: carbohydrate: protein (Research Diets, D12492, New Brunswick, NJ, USA) at 7 weeks old for 16 weeks. Unless otherwise stated, mice were sacrificed after overnight fasting.

All animal procedures were performed in accordance with the Swiss guidelines and were approved by the Canton of Vaud SCAV (authorization VD 3121).

Body composition and indirect calorimetry

The whole-body composition was measured using EchoMRI. Comprehensive Laboratory Animal Monitoring System (CLAMS; Columbus Instruments, Columbus, OH, USA) was used to measure oxygen consumption (VO₂), carbon dioxide production (VCO₂), food intake and water intake. The respiratory exchange ratio (RER) was calculated with VCO₂/VO₂. Energy expenditure (EE) was estimated using VO₂ and VCO₂ values from indirect calorimetry, using the following equation EE (in kcal·h⁻¹) = (3.815 × VO₂) + (1.232 × VCO₂). For the data obtained from HFD-fed mice, the regression comparing VO₂ or EE and body weight was analysed and plotted with CalR [30].

Glucose tolerance test and insulin tolerance test

Mice were fasted overnight before being submitted to a glucose tolerance test (GTT). Chow diet and HFD mice were injected intraperitoneally (i.p.) with 2 and 1.5 g·kg⁻¹ dose glucose respectively. Small drops of tail vein blood were measured at 0', 15', 30', 60', 90', 120' by Accu-Chek[®] Aviva meter (Roche, Basel, Switzerland).

Before the insulin tolerance test (ITT), mice were fasted for 4 h in the morning. According to animal welfare requirements and pretested glycaemia, different insulin (Actrapid, Novo Nordisk, Bagsvaerd, Denmark) doses were administrated as 0.75 U·kg⁻¹ on chow diet-fed young mice; 1.5 U·kg⁻¹ on chow diet-fed aged mice; 2 U·kg⁻¹ on high-fat diet-fed mice.

Serum and liver parameters

Mouse serum parameters were analysed using commercially available reagent kits, such as Wako NEFA-HR(2) reagent (FUJIFILM, Neuss, Germany); Triglycerides FS* (DiaSys, 157609910026, Holzheim, Germany); Free Glycerol Reagent (Sigma-Aldrich, F6428, St. Louis, MO, USA); and Mouse Ultrasensitive Insulin ELISA (ALPCO, 80-INSMSU-E01, Salem, MA, USA). Resistin and leptin levels in serum were assessed by the Mouse Metabolic Evaluation Facility at Center for Integrative Genomics (CIG), University of Lausanne, using a Merck Milliplex Mouse Metabolic kit (Ref. #MMHMAG-44K) on a Luminex 200 system, following the manufacturer's protocol. The free fatty acids (FFAs), triacylglycerol (TG) and cholesterol levels in liver were measured with the same technical services.

Tissue histology

Mouse adipose tissues and liver were fixed in 4% formalin and then sectioned after being paraffin-embedded.

Haematoxylin–eosin (H&E) staining was afterwards performed. Multiple images were analysed with Adiposoft to quantify adipocyte size [31]. The quantification of lipid droplets in H&E-stained liver specimens was performed following the protocol from Ref. [32].

Real-time quantitative PCR analysis

Total mRNA was extracted from tissues using TRI Reagent (Sigma-Aldrich, T9424) according to the manufacturer's protocol. Chloroform was used for phase separation after centrifugation to remove debris (12 000 g, 15 min, 4 °C). The aqueous phase was recovered and precipitated with 100% isopropanol, and centrifuged (12 000 g, 10 min, 4 °C), and RNA pellets were washed with 75% ethanol and resuspended in 200 µL Milli-Q water. A second step of 1 : 1 chloroform was used for further purification. The aqueous phase was recovered and incubated overnight at –20 °C with 1 µL glycogen, 70 µL of ammonium acetate (NH₄AC) and 600 µL of absolute ethanol. After that, the precipitation of RNA pellet was washed with 75% ethanol after centrifugation (12 000 g, 30 min, 4 °C) and then resuspended with Milli-Q water.

RNA concentrations were determined using NanoDrop, and one microgram of the RNA was subsequently reverse-transcribed with SuperScript™ II Reverse Transcriptase (Invitrogen, 18064014, Waltham, MA, USA) according to the manufacturer's instructions. Real-time quantitative PCR was performed using SYBR Green Master Mix (Roche, 04913914001) and ABI 7900HT Fast Real-Time PCR System (Applied Biosystems, Thermo Fisher, Waltham, MA, USA). Fold change was determined by comparing target gene expression with the reference gene *36b4*. Relative mRNA fold changes between groups were calculated using the $\Delta\Delta C_t$ method. The complete list of primers is presented in Table 1.

Western blotting

Protein extraction was isolated with M-PER™ Mammalian Protein Extraction Reagent (Thermo Fisher, 78501) and quantified with Pierce™ BCA Protein Assay Kit (Thermo Fisher, 23225). For western blotting, proteins were separated in a 10% SDS/PAGE and transferred onto nitrocellulose membranes (Bio-Rad, 1620115, Hercules, CA, USA). The following primary antibodies were used in this study: FAS (CST, 3180S, Danvers, MA, USA); p-ACC (Ser79) (Merck, 07-303, Darmstadt, Germany); p-HSL (Ser563) (CST, 4139S, Boston, MA, USA); HSL (SANTA CRUZ, sc-25843); ATGL (CST, 2138S, Boston, MA, USA); Perilipin A (Abcam, ab61682, Cambridgeshire, UK); PPAR γ (CST, 2492); and Tubulin (Sigma, T6199, St. Louis, MO, USA).

Statistical analyses

Data were presented as mean \pm standard error of the mean (SEM). Differences between the two groups were analysed

Table 1. Primer list in qPCR.

Gene	Primer sequence
<i>36b4</i>	F: 5'-AGATTCGGGATATGCTGTGTGG-3' R: 5'-AAAGCCTGGAAGAAGGAGGTC-3'
<i>Adipoq</i>	F: 5'-AAGAAGGACAAGGCCGTTCTCTT-3' R: 5'-GCTATGGGTAGTTGCAGTCAGTT-3'
<i>Pnpla2</i>	F: 5'-AACACCAGCATCCAGTTCAA-3' R: 5'-GGTTCAGTAGGCCATTCTCTC-3'
<i>Cdk7</i>	F: 5'-CAGTTTGCACGGTCTATAA-3' R: 5'-CTCCCTTAAGCTGTTCTATTT-3'
<i>Cebpa</i>	F: 5'-CAGAGGGACTGGAGTTATGA-3' R: 5'-GGACACAGAGACCAGATACA-3'
<i>Cre</i>	F: 5'-ACGTTACCGGCATCAACGT-3' R: 5'-CACGACCAAGTGACAGCAATG-3'
<i>Fabp4</i>	F: 5'-AACACCAGATTTCTCTCAA-3' R: 5'-AGTCACGCCCTTTCATAACACA-3'
<i>Fasn</i>	F: 5'-AATGGCACCTGAACCTTGACA-3' R: 5'-ATATACGCTCCATGGTAGAGTT-3'
<i>Lipe</i>	F: 5'-ACACAAAGCTGCTTCTAC-3' R: 5'-TCTCGTTGCGTTTGTAGTG-3'
<i>Plin1</i>	F: 5'-GTGGAGAGTAAGGATGTCAATG-3' R: 5'-GTGCTGTTGTAGGTCTTCTG-3'
<i>Pparg</i>	F: 5'-CACCAGTGTGAATTACAGCAAATC-3' R: 5'-AGCTGATTCGGAAGTTGGTG-3'

using Student's *t*-test (two-tailed), and multiple comparisons were analysed by ANOVA with a Tukey *post hoc* test. Adipocyte size differences were analysed by the chi-squared test. The differences were considered statistically significant at **P* < 0.05, ***P* < 0.01 and ****P* < 0.001. RNA-seq data from our previous study were analysed using METASCAPE [29,33]. All graphs were generated using GRAPHPAD PRISM 8.2.0 (San Diego, CA, USA).

Results

CDK7 adipose-specific knockout mice have decreased fat mass

A first indication of the participation of CDK7 in WAT physiology came from the transcriptome data that we generated from perigonadal white adipose tissue (pgWAT) in CDK7 fat-specific knockout mice (GSE149128) [29]. Pathway analysis showed that a significant proportion of the 190 downregulated genes (*P* < 0.05, log FC 0.5) that were found in the WAT of the *Cdk7^{fatKO}* mice are involved in lipid metabolism (lipid synthesis, uptake and lipolysis) (Fig. 1A), such as *Fasn*, *Dgat2* and *Lipe* (Table 2).

While the first characterization of the *Cdk7^{fatKO}* mice indicated no difference in body weight compared with *Cdk7^{fl/fl}* mice (Fig. S1A), a more detailed analysis of body composition by EchoMRI analysis showed that *Cdk7^{fatKO}* mice had significantly lower fat mass and

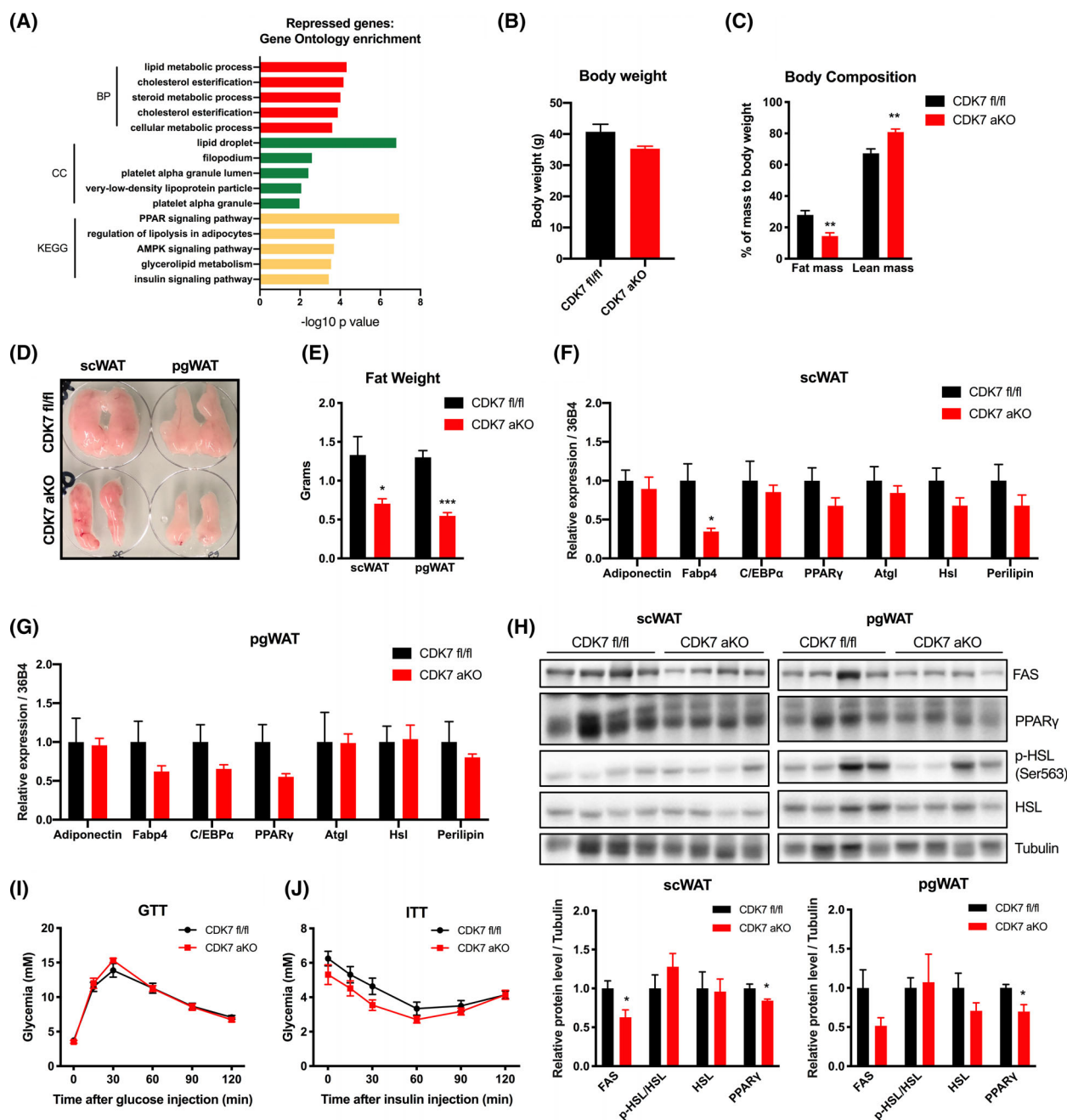


Fig. 1. CDK7 adipocyte-specific knockout mice have less fat mass. (A) Pathway analysis of downregulated genes in pgWAT of *CDK7^{aKO}* versus *CDK7^{fl/fl}* identified by RNA-seq and selected by Enrichr combined score (GO BP, biological process; GO CC, cellular component; and KEGG, Kyoto Encyclopedia of Genes and Genomes). (B, C) Body weight, fat mass and lean mass were analysed by EchoMRI (23-week-old male, $n = 8$ for each group). (D, E) White adipose tissue photographs and weights of male *CDK7^{fl/fl}* and *CDK7^{aKO}* mice (25-week-old male, $n = 6$ for each group). (F, G) Adipogenesis- and lipolysis-related genes in scWAT and pgWAT were analysed by qPCR (25-week-old male, $n = 6$ for each group). (H) Protein levels of FAS, PPAR γ , and phosphorylated and total HSL in scWAT and pgWAT. Tubulin was used as the loading control. Glucose tolerance test (I) and insulin tolerance test (J) of *CDK7^{fl/fl}* and *CDK7^{aKO}* mice (male, 14 weeks old, $n = 7-9$). Values represent means \pm SEM. * $P < 0.05$ and *** $P < 0.001$.

increased lean mass compared with *Cdk7^{fl/fl}* littermates on chow diet (Fig. 1B,C). Consistently, the subcutaneous white adipose tissue (scWAT) and pgWAT

deposits of *Cdk7^{aKO}* were smaller than *Cdk7^{fl/fl}* mice (Fig. 1D,E). Gene and protein expression analyses in the adipose tissue also showed significant differences

Table 2. Selected downregulated genes in pgWAT of *Cdk7^{aKO}* compared with WT in GSE149128.

Function	Gene	log2 fold change	Standard error	P-adj
Lipid synthesis	Scd1	-1.4414	0.2347	4.88E-06
	Scd2	-1.1254	0.2734	0.0029
	Fasn	-0.9618	0.2745	0.0113
	Dgat2	-0.9115	0.1288	0.0001
	Agpat2	-0.8030	0.1803	0.0114
	Mogat2	-0.9452	0.2352	0.0073
Lipid transport	Fabp4	-0.6473	0.1418	0.0372
	Slc27a1	-1.0083	0.0774	3.62E-12
	apoe	-0.6968	0.1726	0.0314
	Apol6	-1.0254	0.0773	4.44E-13
Lipolysis	Lipe	-0.8735	0.1557	0.0019
	Plin1	-0.8262	0.1772	0.0081
	G0s2	-1.1190	0.3220	0.0068
	Plin4	-0.7944	0.1208	0.0018

between genotypes, with decreased *Fabp4* mRNA expression, and FAS and PPAR γ proteins in the *Cdk7^{aKO}* mice (Fig. 1F–H). Consistent with the gene expression, reduced serum concentrations of nonesterified fatty acids (NEFAs) and glycerol in *Cdk7^{aKO}* mice were observed (Fig. S1G–I), suggesting a decreased lipid turnover (decreased lipid synthesis/lipolysis). Serum adipokine measurement showed a reduction in the level of resistin but not leptin in *Cdk7^{aKO}* mice (Figure S1J,K).

Finally, the glucose tolerance test (GTT) and the insulin tolerance test (ITT) were not different between genotypes (Fig. 1I,J), indicating no effects of the deletion of adipose tissue *Cdk7* on systemic metabolism in these conditions. Moreover, *Cdk7^{aKO}* and *Cdk7^{fl/fl}* mice had similar oxygen consumption (VO₂), respiratory exchange ratio (RER), energy expenditure (EE), food intake and physical activity on chow diet (Fig. S1B–F).

Impaired adipose tissue expansion in *Cdk7^{aKO}* mice under HFD

To further investigate the role of CDK7 in adipose tissue expansion, *Cdk7^{fl/fl}* and *Cdk7^{aKO}* mice were fed on HFD. After 10 weeks, *Cdk7^{fl/fl}* mice became markedly obese, whereas *Cdk7^{aKO}* gained significantly less weight (Fig. 2A), which was consistent with decreased fat mass in these mice (Fig. 2B). In addition, the weight of WAT in the different depots in *Cdk7^{aKO}* mice was significantly decreased (Fig. 2C,D). In addition, adipocyte size was also smaller in *Cdk7^{aKO}* than that in *Cdk7^{fl/fl}* (Fig. 2E, F). qPCR and western blotting results demonstrated that adipose markers in scWAT and pgWAT (Fig. 2G–I), including *Adiponectin*, *Ppar γ* , *C/ebp α* , *Hsl* and

Perilipin, were decreased in the adipose tissue of *Cdk7^{aKO}* mice. Consistently, the serum concentrations of leptin and resistin, two well-known adipokines secreted by mature adipocytes, were lower in *Cdk7^{aKO}* mice than in *Cdk7^{fl/fl}* on HFD (Fig. 2J,K).

Insulin resistance in *Cdk7^{aKO}* mice under HFD

When analysing the tissues involved in metabolic control, we found that the size of the liver in *Cdk7^{aKO}* was bigger than in *Cdk7^{fl/fl}* mice under HFD (Fig. 3A), which was confirmed by the marked increase in liver weight (Fig. 3B), with a tendency to contain more lipid droplets (Fig. 3C). These data suggested that the deletion of CDK7 in adipocytes affected systemic metabolism when mice were fed a HFD. Accordingly, ITT indicated that *Cdk7^{aKO}* mice are more insulin-resistant upon HFD (Fig. 3F,G). However, *Cdk7^{aKO}* mice on HFD did not show changes in fasting glycaemia and glucose tolerance (Fig. 3D,E). Decreased adipose tissue mass also resulted in reduced serum concentrations of nonesterified fatty acids (NEFAs), triacylglycerol (TG) and glycerol in *Cdk7^{aKO}* mice (Fig. B–D), suggesting a decreased lipid turnover (decreased lipid synthesis and lipolysis) as indicated by the gene expression analysis. However, no changes were observed in food intake, ambulatory activity, oxygen consumption, RER and energy expenditure (Fig. S2A–E).

Cdk7^{aKO} mice develop insulin resistance upon ageing

Since ageing is also associated with profound changes in adipose tissue and lipid turnover [34], we analysed fat expansion and glucose homeostasis in aged *Cdk7^{aKO}* mice. No significant difference in body weight was observed at 13-month-old mice between genotypes (Fig. 4A); however, aged *Cdk7^{aKO}* mice had smaller white adipose tissue depots and bigger liver size (Fig. 4B,C). The elevated lipid accumulation in *Cdk7^{aKO}* liver was confirmed by histological analysis (Fig. 4D,G). The adipocytes size in *Cdk7^{aKO}* scWAT and pgWAT was smaller than in *Cdk7^{fl/fl}* mice (Fig. 4E,F), which suggested impaired lipid storage capacity. Similar to the phenotype of the *Cdk7^{aKO}* mice fed on HFD, no differences in fasting glycaemia and glucose tolerance were found between both genotypes in aged mice (Fig. 4H,I), while the *Cdk7^{aKO}* mice were more insulin-resistant (Fig. 4J,K). Serum concentrations of NEFA, triacylglycerol and glycerol in aged *Cdk7^{aKO}* mice had a tendency to be lower (Fig. S3F–H). Overall, these data indicated that *Cdk7^{aKO}* mice

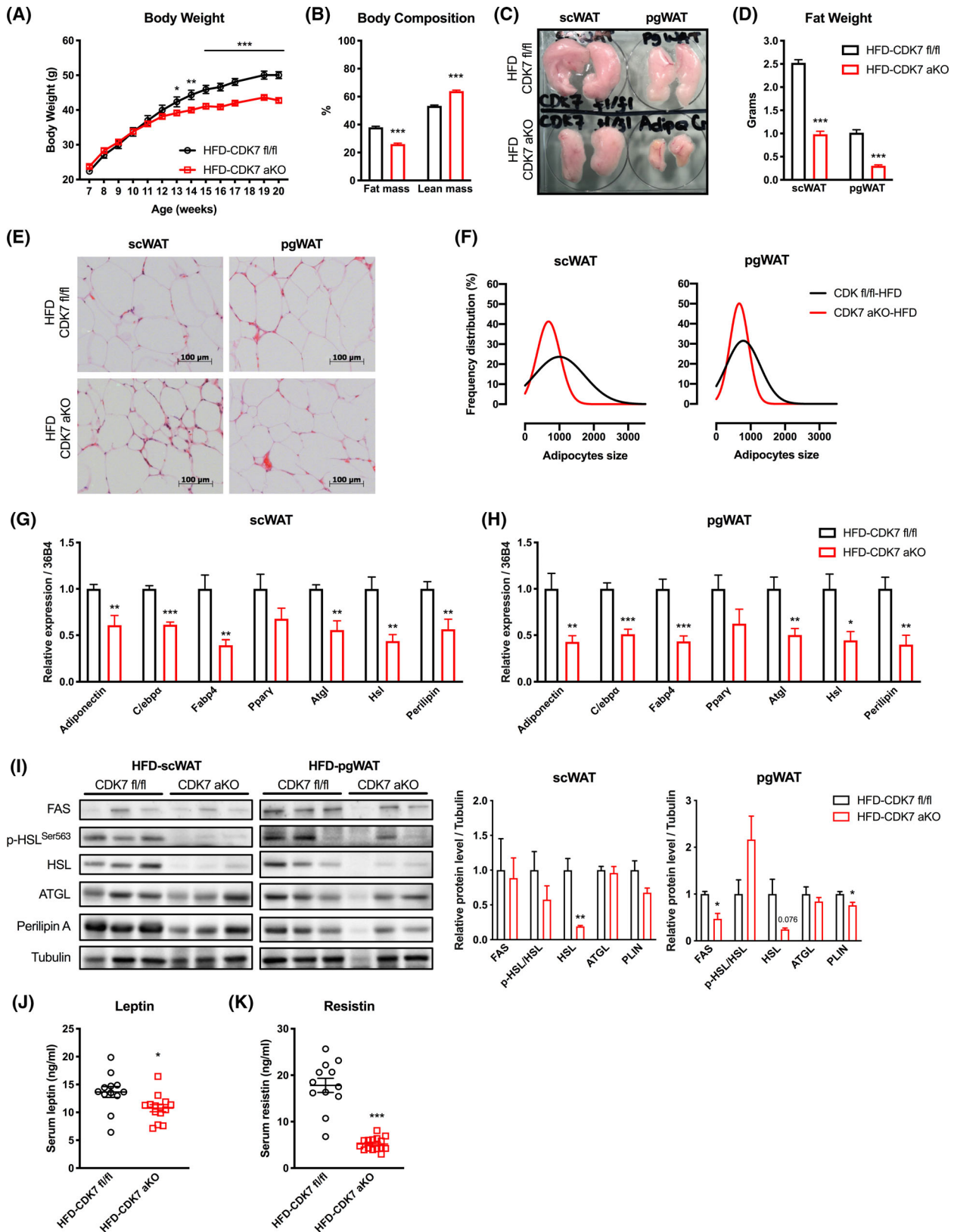


Fig. 2. CDK7 ablation leads to lipodystrophy upon HFD-induced obesity. (A) Body weight curve of male $CDK7^{fl/fl}$ (control) and $CDK7^{aKO}$ mice on high-fat diet ($n = 12-15$ for each group). (B) Fat mass and lean mass of HFD-fed mice were analysed by EchoMRI (23-week-old male, $n = 12-15$ for each group). (C, D) White adipose tissue photographs and weights of $CDK7^{fl/fl}$ and $CDK7^{aKO}$ mice on HFD (male, 25 weeks old, $n = 12-15$ for each group). (E) H&E staining of white adipose tissues of HFD-fed $CDK7^{fl/fl}$ and $CDK7^{aKO}$ mice. Scale bar: 100 μm . (F) Quantification of adipocyte size in white adipose tissues of HFD-fed $CDK7^{fl/fl}$ and $CDK7^{aKO}$ mice. (G, H) Adipogenesis- and lipolysis-related genes in scWAT and pgWAT were analysed by qPCR ($n = 6$). (I) Protein levels of FAS, phosphorylated and total HSL, ATGL and Perilipin in scWAT and pgWAT of HFD-fed $CDK7^{fl/fl}$ and $CDK7^{aKO}$ mice. Tubulin was used as the loading control. Serum leptin (J) and resistin (K) concentrations of HFD-fed $CDK7^{fl/fl}$ and $CDK7^{aKO}$ mice (25-week-old male, $n = 12-15$). Values represent means \pm SEM. * $P < 0.05$, ** $P < 0.01$ and *** $P < 0.001$.

developed a lipodystrophy-like phenotype and insulin resistance upon ageing, similar to the phenotype of the HFD-fed $Cdk7^{aKO}$ mice.

Discussion

In this study, we investigated the role of CDK7 in mature adipocytes by deleting *Cdk7* with the *Adiponectin* promoter-mediated Cre-Lox system. We found that CDK7 fat-specific knockout mice are normal with similar body weight, energy expenditure, insulin sensitivity and

glucose tolerance. However, CDK7 ablation in mature adipocytes leads to decreased fat mass. Moreover, CDK7 adipocyte-specific knockout mice are resistant to HFD-induced obesity. The lean phenotype is not due to increased energy expenditure as demonstrated by indirect calorimetry. Rather, the knockout mice have a defect in adipose tissue expansion, which redistributes lipids to the liver resulting in severe hepatomegaly and hepatic steatosis. Interestingly, the $Cdk7^{aKO}$ mice also appear to have a tendency of increased food intake under HFD (Fig. S2A), which can be explained by decreased leptin secretion

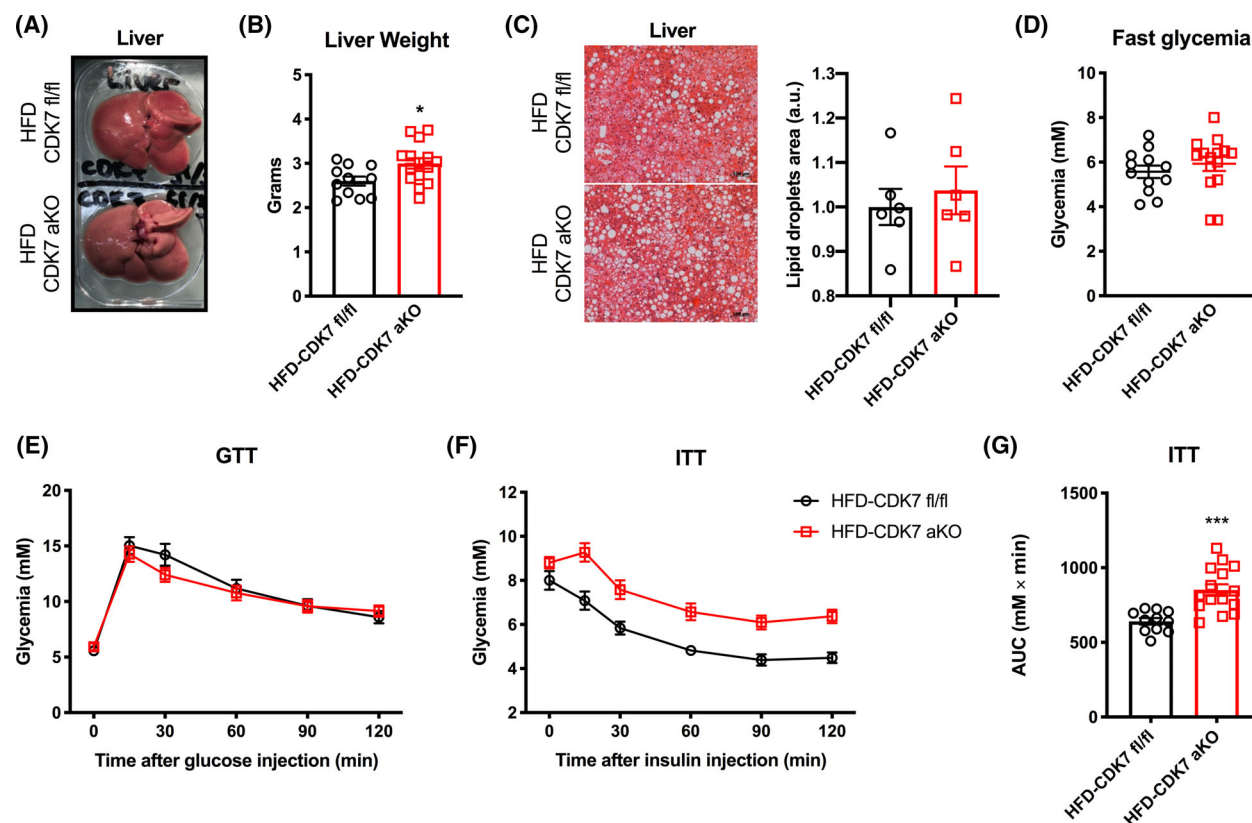


Fig. 3. CDK7 ablation leads to insulin resistance upon high-fat diet. (A, B) Liver photograph and weight of male $CDK7^{fl/fl}$ and $CDK7^{aKO}$ mice on HFD (25 weeks old). (C) H&E staining and its quantification of lipid droplet area of liver of HFD $CDK7^{fl/fl}$ and $CDK7^{aKO}$ mice (male, 25 weeks old, $n = 6$); Scale bar: 100 μm . Fasting glycaemia (D), glucose tolerance test (E), insulin tolerance test (F) and area under the curve (AUC) of ITT (G) of $CDK7^{fl/fl}$ and $CDK7^{aKO}$ mice on HFD (male, 20 weeks old, $n = 12-15$). Values represent means \pm SEM. * $P < 0.05$ and *** $P < 0.001$.

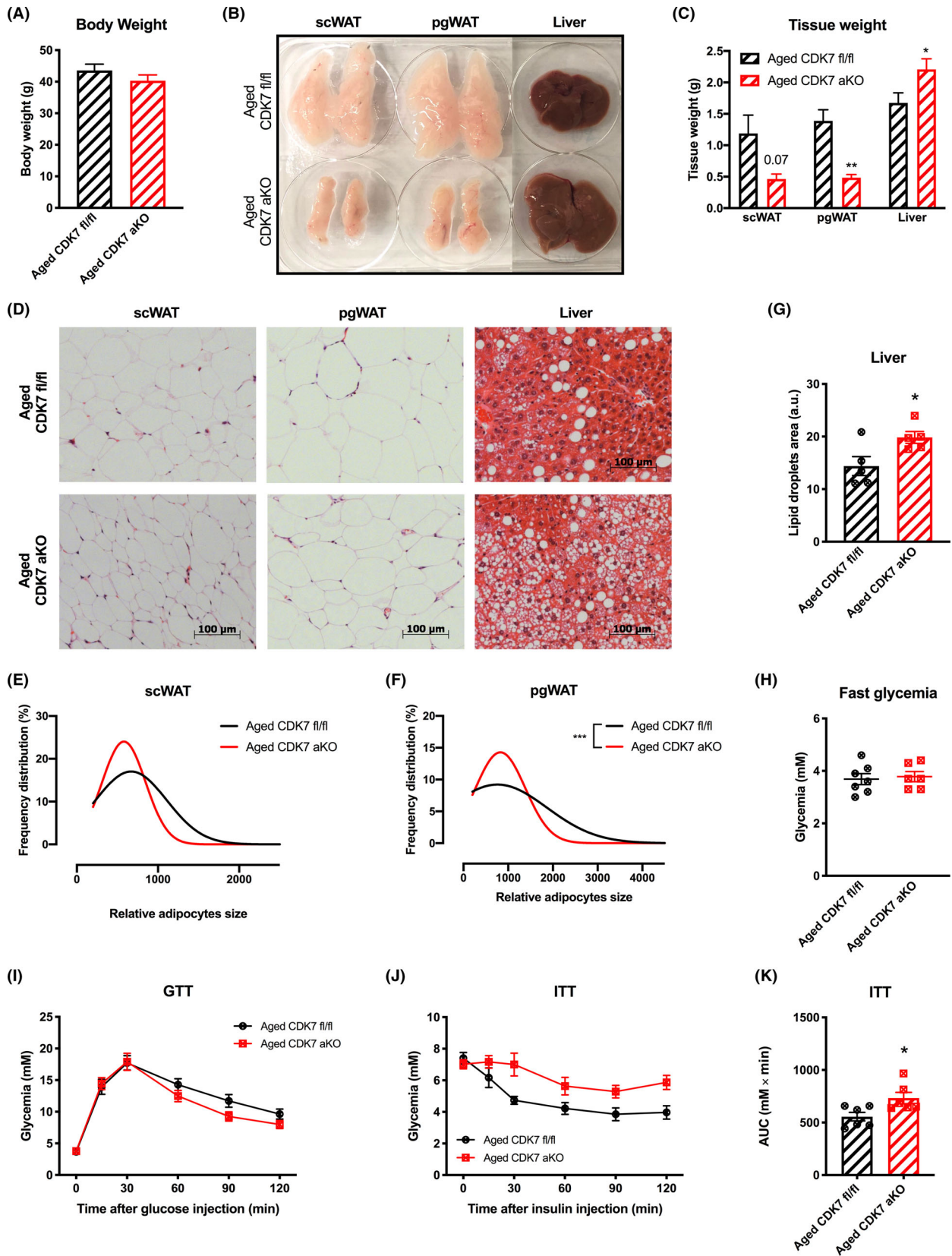


Fig. 4. *CDK7^{akO}* mice develop insulin resistance upon ageing. (A) Body weight of old *CDK7^{fl/fl}* and *CDK7^{akO}* mice on chow diet (male, 56 weeks old, $n = 5-8$). Adipose tissues and liver photographs (B), weights (C) and H&E staining (D) of old *CDK7^{fl/fl}* and *CDK7^{akO}* mice (male, 56 weeks old). (E, F) Quantification of adipocyte size in scWAT and pgWAT of aged *CDK7^{fl/fl}* and *CDK7^{akO}* mice. (G) Quantification of lipid droplets in H&E-stained liver of aged *CDK7^{fl/fl}* and *CDK7^{akO}* mice (male, 56 weeks old, $n = 5$). Fasting glycaemia (H), glucose tolerance test (I), insulin tolerance test (J) and area under the curve (AUC) of ITT (K) of old *CDK7^{fl/fl}* and *CDK7^{akO}* mice (male, 49 weeks old, $n = 6-7$). Values represent means \pm SEM. * $P < 0.05$ and ** $P < 0.01$.

(Fig. 2J). According to energy balance, the leaner *Cdk7^{akO}* mice did not eat less or expend more energy; it is reasonable to speculate that the *Cdk7^{akO}* mice have a defect in dietary lipid absorption in the intestine. This mild lipodystrophy phenotype is exacerbated in ageing *Cdk7^{akO}* mice, even when fed a chow diet. In addition to decreased fat mass, the *Cdk7^{akO}* mice are also insulin-resistant under HFD and during ageing. However, in both conditions, fasting glycaemia and glucose tolerance were not changed (Figs 3D,E and 4H,I), which could be explained by a compensatory effect. Indeed, we found an increase in insulin secretion in *Cdk7^{akO}* mice under fasting conditions (Fig. S3A,E), which also demonstrates that *Cdk7*-specific ablation in adipose tissue can alter systemic metabolic homeostasis in the liver and pancreas.

Cdk7 full-body knockout leads to embryonic lethality in mice [35]; however, tamoxifen-induced *Cdk7* knockout in adult tissues resulted in body weight loss [35], which suggested a potential link between *Cdk7* and adipose tissue. Moreover, these mice were deficient in subcutaneous adipose tissue [35]. More evidence in support of a role of CDK7 in adipose tissue came from the finding that patients with mutations in the XPD subunit of TFIIH, from which CDK7 is a subunit, develop clinical hypoplasia of the adipose tissue. It was proposed that in adipose tissue, the XPD mutation could impact CDK7 activity towards PPAR γ , a master regulator of adipogenesis [36]. Indeed, PPAR γ is a validated target of CDK7. In contrast to these studies, it was reported that *Mat1* (partner of CDK7)-deficient mouse embryonic fibroblasts have improved adipogenesis through the decrease in inhibitory PPAR γ phosphorylation by CDK7 [37]. It is still possible that MAT1 has some CDK7-independent effects that could explain this controversy.

It is still unclear how CDK7 specifically regulates lipid metabolism genes in mature adipocytes. CDK7 functions as a CAK during cell cycle progression [13,14] and also as an essential component of the transcription factor TFIIH, which is involved in transcriptional initiation [15]. As a CAK, CDK7 is required to maintain the active state of CDK4 through the phosphorylation of the T-loop site during the cell cycle [38]. A study by us and others found that cell cycle regulators are involved in many aspects of metabolism regulation [19]. In mature adipocytes, CDK4

can be activated by insulin and mediates insulin signalling by phosphorylation of insulin receptor substrate 2 (IRS2) [21]. The lean but insulin-resistant phenotypes observed especially in HFD-induced obesity and ageing *Cdk7^{akO}* mice resemble that of CDK4 knockout mice, even though in a milder way. It is reasonable to speculate that under anabolic conditions, CDK7 may exert its effects on adipocytes by modulating CDK4 activity. However, upon ageing CDK4 KO mice have a complete loss of adipose tissue (unpublished data), suggesting that CDK4 is activated by other mechanisms in addition to CDK7 in this tissue under these conditions.

Several CDK7 inhibitors have been in clinical trials for cancer treatment [39–42]. Based on our study, it will be also important to evaluate their potential metabolic effect, especially on obese and old patients. Collectively, our findings offer new insights into the essential role of CDK7 in WAT expansion, especially upon HFD and during ageing.

Acknowledgements

The authors acknowledge all the members of the Fajas laboratory for support and discussions. The authors thank Frédéric Preitner, Gilles Willemin and Guy Niederhäuser from Mouse Metabolic Facility of CIG (University of Lausanne, Switzerland) for experimental assistance. We thank M. Barbacid and D. Santamaria (CNIO, Spain) for providing the *Cdk7* flox mice.

Data accessibility

The RNA-seq data are openly available in a public repository with the <https://doi.org/10.1016/j.isci.2020.101163>.

Author contributions

LFC and HJ conceptualized and supervised the study. YC, HJ, EAF, CR and ICLM investigated the study. ICLM and LFC provided resources. YC and HJ developed methodology, performed data curation, wrote and prepared the original draft. YC, ILCM, LFC and HJ wrote, reviewed and edited the manuscript. LFC acquired funding.

Funding

Yizhe Chen and Honglei Ji were supported by scholarship (No. 201706300109 and No. 201406300121) from China Scholarship Council. IC Lopez-Mejia was supported by an SNSF Ambizione Grant (PZ00P3_168077). This research from Prof. Fajas laboratory is funded by the Swiss National Foundation, grant number 179271.

Institutional review board statement

All animal procedures were performed in accordance with the Swiss guidelines and were approved by the Canton of Vaud SCAV (authorization VD 3121).

References

- Krahmer N, Guo Y, Farese RV Jr, Walther TC. SnapShot: lipid droplets. *Cell*. 2009;**139**:1024–1024.e1021. <https://doi.org/10.1016/j.cell.2009.11.023>
- Deng Y, Scherer PE. Adipokines as novel biomarkers and regulators of the metabolic syndrome. *Ann N Y Acad Sci*. 2010;**1212**:E1–E19. <https://doi.org/10.1111/j.1749-6632.2010.05875.x>
- Abella V, Scotece M, Conde J, López V, Lazzaro V, Pino J, et al. Adipokines, metabolic syndrome and rheumatic diseases. *J Immunol Res*. 2014;**2014**:343746. <https://doi.org/10.1155/2014/343746>
- Luo L, Liu M. Adipose tissue in control of metabolism. *J Endocrinol*. 2016;**231**:R77–99. <https://doi.org/10.1530/joe-16-0211>
- Castillo-Armengol J, Fajas L, Lopez-Mejia IC. Inter-organ communication: a gatekeeper for metabolic health. *EMBO Rep*. 2019;**20**:e47903. <https://doi.org/10.15252/embr.201947903>
- Ganda OP. Lipoatrophy, lipodystrophy, and insulin resistance. *Ann Intern Med*. 2000;**133**:304–6. <https://doi.org/10.7326/0003-4819-133-4-200008150-00017>
- Lee PL, Tang Y, Li H, Guertin DA. Raptor/mTORC1 loss in adipocytes causes progressive lipodystrophy and fatty liver disease. *Mol Metab*. 2016;**5**:422–32. <https://doi.org/10.1016/j.molmet.2016.04.001>
- Garg A. Lipodystrophies: genetic and acquired body fat disorders. *J Clin Endocrinol Metab*. 2011;**96**:3313–25. <https://doi.org/10.1210/jc.2011-1159>
- Hussain I, Garg A. Lipodystrophy syndromes. *Endocrinol Metab Clin North Am*. 2016;**45**:783–97. <https://doi.org/10.1016/j.ecl.2016.06.012>
- Akinci B, Sahinoz M, Oral E. Lipodystrophy syndromes: presentation and treatment. In: Feingold KR, Anawalt B, Boyce A, Chrousos G, de Herder WW, Dhatariya K, Dungan K, Hershman JM, Hofland J, Kalra S, Kaltsas G, Koch C, Kopp P, Korbonits M, Kovacs CS, Kuohung W, Laferrère B, Levy M, McGee EA, McLachlan R, Morley JE, New M, Purnell J, Sahay R, Singer F, Sperling MA, Stratakis CA, Trencle DL, Wilson DP, editors. *Endotext*. South Dartmouth, MA: MDText.com, Inc.; 2000.
- Malumbres M. Cyclin-dependent kinases. *Genome Biol*. 2014;**15**:122. <https://doi.org/10.1186/gb4184>
- Lim S, Kaldis P. Cdks, cyclins and CKIs: roles beyond cell cycle regulation. *Development*. 2013;**140**:3079–93. <https://doi.org/10.1242/dev.091744>
- Makela TP, Tassan JP, Nigg EA, Frutiger S, Hughes GJ, Weinberg RA. A cyclin associated with the CDK-activating kinase MO15. *Nature*. 1994;**371**:254–7. <https://doi.org/10.1038/371254a0>
- Yee A, Nichols MA, Wu L, Hall FL, Kobayashi R, Xiong Y. Molecular cloning of CDK7-associated human MAT1, a cyclin-dependent kinase-activating kinase (CAK) assembly factor. *Cancer Res*. 1995;**55**:6058–62.
- Kaldis P. The cdk-activating kinase (CAK): from yeast to mammals. *Cell Mol Life Sci*. 1999;**55**:284–96. <https://doi.org/10.1007/s000180050290>
- Huber K, Mestres-Arenas A, Fajas L, Leal-Esteban LC. The multifaceted role of cell cycle regulators in the coordination of growth and metabolism. *FEBS J*. 2021;**288**:3813–33. <https://doi.org/10.1111/febs.15586>
- Fajas L. Re-thinking cell cycle regulators: the cross-talk with metabolism. *Front Oncol*. 2013;**3**:4. <https://doi.org/10.3389/fonc.2013.00004>
- Aguilar V, Fajas L. Cycling through metabolism. *EMBO Mol Med*. 2010;**2**:338–48. <https://doi.org/10.1002/emmm.201000089>
- Lopez-Mejia IC, Castillo-Armengol J, Lagarrigue S, Fajas L. Role of cell cycle regulators in adipose tissue and whole body energy homeostasis. *Cell Mol Life Sci*. 2018;**75**:975–87. <https://doi.org/10.1007/s00018-017-2668-9>
- Abella A, Dubus P, Malumbres M, Rane SG, Kiyokawa H, Sicard A, et al. Cdk4 promotes adipogenesis through PPARgamma activation. *Cell Metab*. 2005;**2**:239–49. <https://doi.org/10.1016/j.cmet.2005.09.003>
- Lagarrigue S, Lopez-Mejia IC, Denechaud PD, Escoté X, Castillo-Armengol J, Jimenez V, et al. CDK4 is an essential insulin effector in adipocytes. *J Clin Invest*. 2016;**126**:335–48. <https://doi.org/10.1172/jci81480>
- Sarruf DA, Iankova I, Abella A, Assou S, Miard S, Fajas L. Cyclin D3 promotes adipogenesis through activation of peroxisome proliferator-activated receptor gamma. *Mol Cell Biol*. 2005;**25**:9985–95. <https://doi.org/10.1128/mcb.25.22.9985-9995.2005>
- Castillo-Armengol J, Barquissau V, Geller S, Ji H, Severi I, Venema W, et al. Hypothalamic CDK4 regulates thermogenesis by modulating sympathetic innervation of adipose tissues. *EMBO Rep*. 2020;**21**:e49807. <https://doi.org/10.15252/embr.201949807>

- 24 Fajas L, Landsberg RL, Huss-Garcia Y, Sardet C, Lees JA, Auwerx J. E2Fs regulate adipocyte differentiation. *Dev Cell*. 2002;**3**:39–49. [https://doi.org/10.1016/s1534-5807\(02\)00190-9](https://doi.org/10.1016/s1534-5807(02)00190-9)
- 25 Haim Y, Blüher M, Slutsky N, Goldstein N, Klötting N, Harman-Boehm I, et al. Elevated autophagy gene expression in adipose tissue of obese humans: a potential non-cell-cycle-dependent function of E2F1. *Autophagy*. 2015;**11**:2074–88. <https://doi.org/10.1080/15548627.2015.1094597>
- 26 Choi Y, Jang S, Choi MS, Ryoo ZY, Park T. Increased expression of FGF1-mediated signaling molecules in adipose tissue of obese mice. *J Physiol Biochem*. 2016;**72**:157–67. <https://doi.org/10.1007/s13105-016-0468-6>
- 27 Denechaud PD, Fajas L, Giral A. E2F1, a novel regulator of metabolism. *Front Endocrinol*. 2017;**8**:311. <https://doi.org/10.3389/fendo.2017.00311>
- 28 Kahoul Y, Oger F, Moutaigne J, Froguel P, Breton C, Annicotte JS. Emerging roles for the INK4a/ARF (CDKN2A) locus in adipose tissue: implications for obesity and type 2 diabetes. *Biomolecules*. 2020;**10**:1350. <https://doi.org/10.3390/biom10091350>
- 29 Ji H, Chen Y, Castillo-Armengol J, Dreos R, Moret C, Niederhäuser G, et al. CDK7 mediates the beta-adrenergic signaling in thermogenic brown and white adipose tissues. *iScience*. 2020;**23**:101163, doi:<https://doi.org/10.1016/j.isci.2020.101163>
- 30 Mina AI, LeClair RA, LeClair KB, Cohen DE, Lantier L, Banks AS. CalR: a web-based analysis tool for indirect calorimetry experiments. *Cell Metab*. 2018;**28**:656–666.e651. <https://doi.org/10.1016/j.cmet.2018.06.019>
- 31 Galarraga M, Campion J, Munoz-Barrutia A, Boque N, Moreno H, Martinez JA, et al. Adiposoftware: automated software for the analysis of white adipose tissue cellularity in histological sections. *J Lipid Res*. 2012;**53**:2791–6. <https://doi.org/10.1194/jlr.D023788>
- 32 Piao D, Ritchey JW, Holyoak GR, Wall CR, Sultana N, Murray JK, et al. In vivo percutaneous reflectance spectroscopy of fatty liver development in rats suggests that the elevation of the scattering power is an early indicator of hepatic steatosis. *J Innov Opt Health Sci*. 2018;**11**:1850019. <https://doi.org/10.1142/s1793545818500190>
- 33 Zhou Y, Zhou B, Pache L, Chang M, Khodabakhshi AH, Tanaseichuk O, et al. Metascape provides a biologist-oriented resource for the analysis of systems-level datasets. *Nat Commun*. 2019;**10**:1523. <https://doi.org/10.1038/s41467-019-09234-6>
- 34 Arner P, Bernard S, Appelsved L, Fu KY, Andersson DP, Salehpour M, et al. Adipose lipid turnover and long-term changes in body weight. *Nat Med*. 2019;**25**:1385–9. <https://doi.org/10.1038/s41591-019-0565-5>
- 35 Ganuza M, Sáiz-Ladera C, Cañamero M, Gómez G, Schneider R, Blasco MA, et al. Genetic inactivation of Cdk7 leads to cell cycle arrest and induces premature aging due to adult stem cell exhaustion. *EMBO J*. 2012;**31**:2498–510. <https://doi.org/10.1038/emboj.2012.94>
- 36 Compe E, Drané P, Laurent C, Diderich K, Braun C, Hoeijmakers JH, et al. Dysregulation of the peroxisome proliferator-activated receptor target genes by XPD mutations. *Mol Cell Biol*. 2005;**25**:6065–76. <https://doi.org/10.1128/mcb.25.14.6065-6076.2005>
- 37 Helenius K, Yang Y, Alasaari J, Mäkelä TP. Mat1 inhibits peroxisome proliferator-activated receptor gamma-mediated adipocyte differentiation. *Mol Cell Biol*. 2009;**29**:315–23. <https://doi.org/10.1128/mcb.00347-08>
- 38 Schachter MM, Merrick KA, Larochelle S, Hirschi A, Zhang C, Shokat KM, et al. A Cdk7-Cdk4 T-loop phosphorylation cascade promotes G1 progression. *Mol Cell*. 2013;**50**:250–60. <https://doi.org/10.1016/j.molcel.2013.04.003>
- 39 Rimel JK, Poss ZC, Erickson B, Maas ZL, Ebmeier CC, Johnson JL, et al. Selective inhibition of CDK7 reveals high-confidence targets and new models for TFIIF function in transcription. *Genes Dev*. 2020;**34**:1452–73. <https://doi.org/10.1101/gad.341545.120>
- 40 Zhang H, Christensen CL, Dries R, Oser MG, Deng J, Diskin B, et al. CDK7 inhibition potentiates genome instability triggering anti-tumor immunity in small cell lung cancer. *Cancer Cell*. 2020;**37**:37–54.e39. <https://doi.org/10.1016/j.ccell.2019.11.003>
- 41 Kwiatkowski N, Zhang T, Rahl PB, Abraham BJ, Reddy J, Ficarro SB, et al. Targeting transcription regulation in cancer with a covalent CDK7 inhibitor. *Nature*. 2014;**511**:616–20. <https://doi.org/10.1038/nature13393>
- 42 Chipumuro E, Marco E, Christensen CL, Kwiatkowski N, Zhang T, Hatheway CM, et al. CDK7 inhibition suppresses super-enhancer-linked oncogenic transcription in MYCN-driven cancer. *Cell*. 2014;**159**:1126–39. <https://doi.org/10.1016/j.cell.2014.10.024>

Supporting information

Additional supporting information may be found online in the Supporting Information section at the end of the article.

Fig. S1. Indirect calorimetry analysis of *CDK7^{fl/fl}* and *CDK7^{aKO}* mice on chow diet.

Fig. S2. Indirect calorimetry analysis of *CDK7^{fl/fl}* and *CDK7^{aKO}* mice on high fat diet.

Fig. S3. Serum parameters of *CDK7^{fl/fl}* and *CDK7^{aKO}* mice.